

Supporting Information — Interface & confinement induced order and orientation in thin films of Poly- ϵ -caprolactone

Wilhelm Kossack,^{*,†} Anne Seidlitz,[‡] Thomas Thurn-Albrecht,[‡] and Friedrich Kremer[†]

[†]*Universität Leipzig, Fakultät für Physik und Geowissenschaften, Linnéstr. 5, 04103 Leipzig*

[‡]*Martin-Luther-Universität Halle-Wittenberg, Institut für Physik, FG Experimentelle Polymerphysik, 06120 Halle/Saale*

E-mail: wilhelm.kossack@physik.uni-leipzig.de

SI Molecular order

The deviation from the \hat{z} -axis (Θ) of the principal axis of orientation of the different crystal axes, as well as the order parameter S_{ext} along \hat{z} are given in tab. 1. In this context Θ can be understood as the azimuthal angle of a spherical coordinate system: $\Theta = 0^\circ$ refers to the surface normal \hat{z} . The extraordinary axes of orientation do not differ from the surface normal within margins of uncertainty, which grow with decreasing order.

SI Spherulite diameters

The distribution of the diameters, d_S , of the spherulites is determined from micrographs at several positions of the different films. For sample **I308** (crystallized at $T_x = 308$ K) no

Table 1: Results from IR-TMOA and XRD pole figures for supported PCL-films crystallized at different temperatures T_x given in K; The table shows the uniaxial order parameters S_{ext} in units of 10^{-2} describing the alignment along the film normal. The direction of the extraordinary axis of the orientation distribution is given as azimuthal angle of a spherical coordinate system in $^\circ$. In cases where S_{ext} is close to zero, no extraordinary direction, and hence, no Θ can be defined. S_{ext} of the [110]- and [200]-directions (XRD) are based on the assumption of a uniaxial distribution around the surface normal. Their uncertainty is at least 20×10^{-2} (*cf.* manuscript). For $T_x \leq 308$ K no pole distributions were obtained, because of the lateral inhomogeneities and because assessment and IR-TMOA measurements did not suggest considerable orientation.

T_x	$\nu_{1c}(\text{COC})$		$\nu'_{1c}(\text{COC})$		$\nu''_{1a}(\text{COC})$		$\nu_{2c}(\text{COC})$		$\nu_c(\text{CH}_2)$		[110]	[200]
	S_{ext}	Θ	S_{ext}	Θ	S_{ext}	Θ	S_{ext}	Θ	S_{ext}	Θ	S_{ext}	
≤ 333	-18 ± 5	2 ± 5					46 ± 7	3 ± 5				
323	-17 ± 5	2 ± 4	14 ± 5	2 ± 5	-7 ± 5	11 ± 13	26 ± 7	1 ± 3	-26 ± 5	2 ± 5	-22	9
318	-21 ± 6	5 ± 4	13 ± 5	3 ± 3	-11 ± 10	7 ± 6	25 ± 5	2 ± 4	-20 ± 6	5 ± 4	-17	7
313	-5 ± 5	6 ± 7	5 ± 5	13 ± 15	-5 ± 5	2 ± 20	14 ± 5	0 ± 5	-5 ± 5	7 ± 8	-4	2
308	1 ± 4	/	-2 / ± 3	19 ± 20	7 ± 6	3 ± 10	-1 ± 4	/	-4 ± 5	4 ± 15		
303	-6 ± 5	22 ± 20	-6 ± 5	10 ± 10	-6 ± 5	7 ± 15	-4 ± 5	28 ± 15	-3 ± 5	20 ± 15		

distribution is obtained, as the spatial resolution of our microscope is not sufficient to resolve the exact diameters of the structures. Film **NI333** exhibits spherulites with a diameter in the range of 400–500 μm . The corresponding variations of $d_S/h \in [36, 45]$ can be neglected for the model presented in the body of the main text, because they lead to variations of the order parameter of the crystallites smaller than 0.01.¹

SI Atomic Force Microscopy

An Atomic Force Microscopy (AFM) amplitude picture of PCL is shown in fig. 2, resembling the pictures published by Kajioaka et al.^{1,2} This corroborates the identification of the structures seen in the micrographs of PCL-films (*cf.* manuscript) with non-banded spherulites. In

¹Such a variation of d_S has no impact on the order of the crystallites, as their growth is confined very effectively to the sample plane for $d_S/h > 20$.

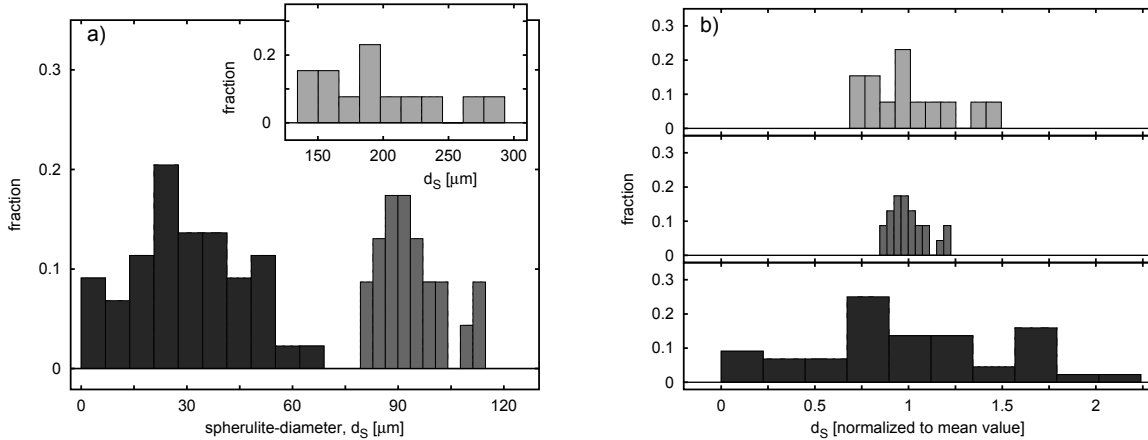


Figure 1: Histograms of spherulite’s diameters; Dark, light and very light grey refer to $T_x = 313$ K, 318 K and 323 K. Panel (b) shows the data of (a) normalized to the respective average spherulite diameter.

particular, edge on lamellae with a characteristic distance of about 300–600 nm are observed, that deviate by up to 45° from the growth direction, and are separated by notches of about 50 nm (fig. 2). But also flat regions can be seen indicating the presence of flat on lamellae at the free interface. The boundaries between spherulites exhibit a drop in depth of ~ 300 nm.

The diameter, d_S , of the spherulites depends on the crystallization temperature T_x . Histograms of d_S for $T_x = 313$ K, 318 K and 323 K are given in fig. 3.

SI Model of a confined spherulite

The modelling of the confined spherulite is depicted in fig. 4. As IR and XRD measure macroscopic averages of the orientation, a periodic (banded) or random (non-banded spherulite) rotation of the crystallites around the growth direction ($[010]$) can be modelled by distributing the $[100]$, $[110]$ and $[001]$ directions on a cone around $[010]$.

Flat on lamellae at the surface serving as a spherulite’s nucleus, and dominating the orientation of the overgrowing lamellae, are modelled by restraining the $[100]$ directions to the $\hat{x}\text{-}\hat{y}$ -plane (fig. 4). In very thin films (~ 100 nm), this leads to two-dimensional spherulites as reported by Mareau and Prud’homme.³ An analogous model is used for edge on lamellae,

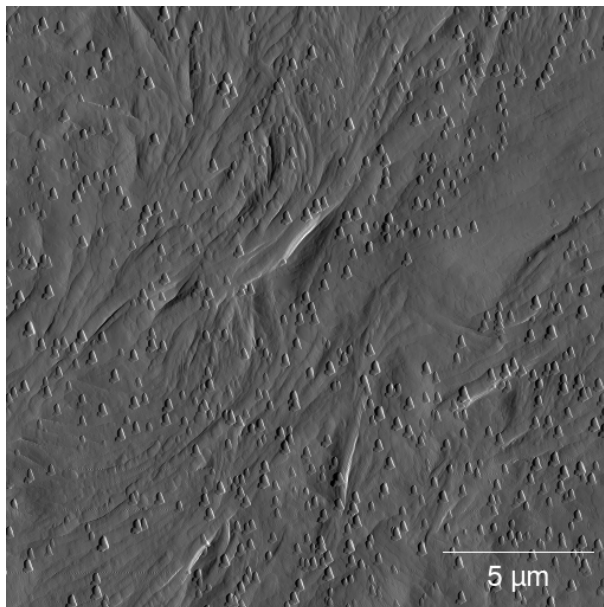


Figure 2: AFM amplitude picture recorded close to the centre of a single spherulite; The small regular structures are artefacts resulting from particles smaller than the AFM-tip. Irregular structures resembling the twisted lamellar arrangement can be seen as well.¹

where the [001]-direction is confined to the \hat{x} - \hat{y} -plane.

Branching is modelled by distributing the [010] vectors (growth direction) on a cone of opening angle ξ around the radius. ξ is chosen randomly for each infinitesimal integration volume based on a probability distribution (fig. 3) extracted from AFM pictures (*e.g.* fig. 2).

References

- (1) Kajioka, H.; Hikosaka, M.; Taguchi, K.; Toda, A. *Polymer* **2008**, *49*, 1685–1692.
- (2) Kajioka, H.; Yoshimoto, S.; Gosh, R. C.; Taguchi, K.; Tanaka, S.; Toda, A. *Polymer* **2010**, *51*, 1837–1844.
- (3) Mareau, V. H.; Prud'homme, R. E. *Macromolecules* **2005**, *38*, 398–408.

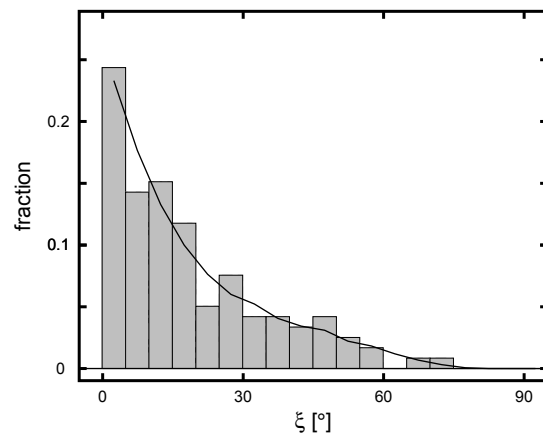


Figure 3: Probability to find an angle ξ of the the local growth direction with the radial direction in the AFM-picture (fig. 4). The line represents the smoothed dependence (Savitzky-Golay filter) used for the model.

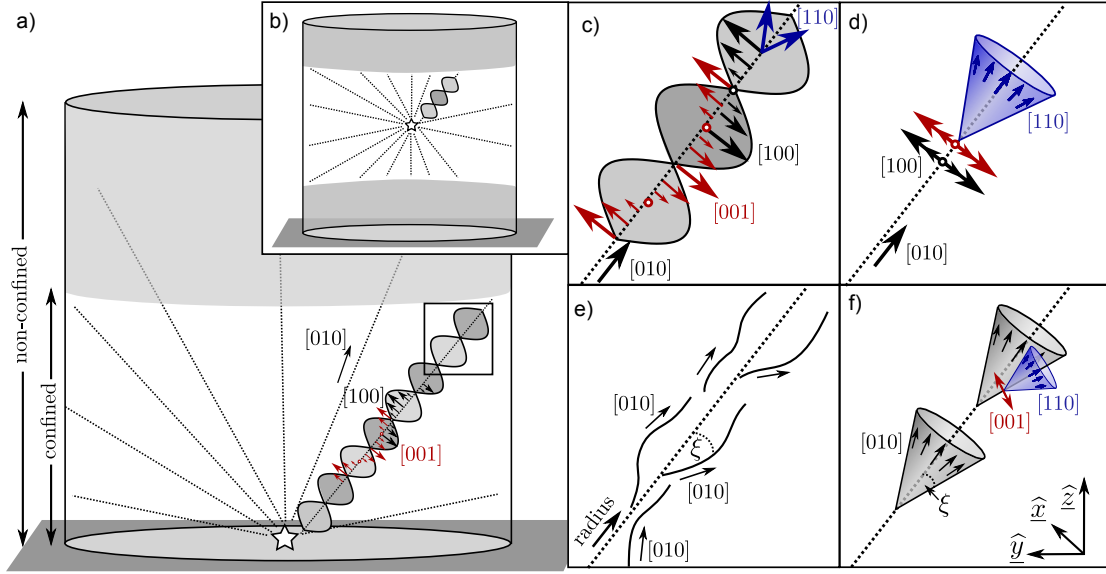


Figure 4: A banded spherulite confined to a cylinder; Confinement by the film thickness is indicated by the grey shaded areas, which are not accessible in thinner films. If the spherulite nucleates (star) at the substrate (a), or in the cylinder's centre (b), its growth is confined in a different way. In a banded spherulite, the $[100]$ (black) and $[001]$ (red) and $[110]$ directions (blue arrows) rotate in a periodic fashion around the $[010]$ growth direction (a, c). In a macroscopic average this can be represented by a distribution of them on a cone around $[010]$ (d). Because of branching and splaying, the growth direction is not exactly radial (e, cf. fig. 2). This is modelled by distributing these vectors on a cone of opening angle ξ around the radius. Around that cone the other lattice directions are distributed (f). Note, that neither IR nor XRD distinguish between banded and non-banded spherulites because of the macroscopic, spatial averaging inherent to both techniques. Consequently, variations of the lattice vectors' orientation along the radius of the spherulite (c, e) are treated as orientation distributions within each infinitesimal integration volume (d, f) in the presented model. The coordinate system is indicated by $\hat{x}, \hat{y}, \hat{z}$.